

Fast cross-validation for multi-penalty ridge regression

Mark A. van de Wiel^{*1,2}, Mirrelijm M. van Nee¹, Armin Rauschenberger³

¹*Department of Epidemiology and Data Science, Amsterdam University Medical Centers, Amsterdam, Netherlands;* ²*MRC Biostatistics Unit, University of Cambridge, Cambridge, UK;* ³*Luxembourg Centre for Systems Biomedicine (LCSB), University of Luxembourg, Esch-sur-Alzette, Luxembourg*

Prediction based on multiple high-dimensional data types needs to account for the potentially strong differences in predictive signal. Ridge regression is a simple, yet versatile and interpretable model for high-dimensional data that has challenged the predictive performance of many more complex models and learners, in particular in dense settings. Moreover, it allows using a specific penalty per data type to account for differences between those. Then, the largest challenge for multi-penalty ridge is to optimize these penalties efficiently in a cross-validation (CV) setting, in particular for GLM and Cox ridge regression, which require an additional loop for fitting the model by iterative weighted least squares (IWLS). Our main contribution is a computationally very efficient formula for the multi-penalty, sample-weighted hat-matrix, as used in the IWLS algorithm. As a result, nearly all computations are in the low-dimensional sample space. We show that our approach is several orders of magnitude faster than more naive ones.

We developed a very flexible framework that includes prediction of several types of response, allows for unpenalized covariates, can optimize several performance criteria and implements repeated CV. Moreover, extensions to pair data types and to allow a preferential order of data types are included and illustrated on several cancer genomics survival prediction problems. The corresponding R-package, `multiridge`, serves as a versatile standalone tool, but also as a fast benchmark for other more complex models and multi-view learners.

1 Introduction

Many researchers face the challenge of integrating multiple (high-dimensional) data types into one predictive model. For example, in many clinical studies multiple genomics types, such as mutations, gene expression and DNA copy number, are measured for the same individuals. A common task then is to build a model for diagnosing disease or predicting therapy response (both binary outcomes), or for predicting survival. The various data types may differ strongly in predictive signal, which demands a multi-view approach to prediction models. We propose a versatile, computationally efficient framework based on multi-penalty ridge regression.

Ridge regression (Hoerl and Kennard, 1970) is one of the oldest statistical models to deal with high-dimensionality. Unlike the more recent sparse methods, it does not select features although posterior selection can be applied (Bondell and Reich, 2012; Perrakis et al., 2019). Moreover, others have argued that many diseases are likely poly- or even omnigenic (Boyle et al., 2017), which in combination with high collinearity, may render sparse methods sub-optimal in terms of prediction. The relative good predictive performance of ridge regression compared to several other methods, including its sparse counterpart, lasso, is confirmed in (Bernau et al., 2014) for several genomics applications. On the other side of the spectrum, very dense multi-view deep learners are data hungry in terms of sample size, conflicting with the small n setting in many clinical genomics studies (often $n < 100$ or several hundreds at most), and do not necessarily outperform much simpler models for relatively large genomics data sets either (see Warnat-Herresthal et al., 2020, $n \approx 8,000$). Moreover, unlike for many more complicated models, the analytical tractability of ridge regression allows theoretical

results on predictive risks (Dobriban and Wager, 2018) and model diagnostics (Özkale et al., 2018). Finally, the predictive performance of ridge regression can be boosted by incorporating different penalties for groups of features (Van de Wiel et al., 2016; Velten and Huber, 2018; Perrakis et al., 2019).

Our approach aligns with the latter works: it allows different penalties for different data types. The estimation of these, however, is fully based on cross-validation (CV) instead of (empirical) Bayes, rendering the method very generic in terms of i) the response and corresponding model (linear, logistic, Cox); ii) potential inclusion of non-penalized clinical covariates; and iii) evaluation score, such as log-likelihood, area-under-the-roc-curve, and c-index. CV for multiple penalty parameters is computationally demanding, so our aim is to overcome this hurdle. Therefore, we developed `multiridge`: a method for efficient estimation of multiple penalties by fully exploiting the algebraic properties of the (iterative) ridge estimator. We first shortly review fast CV for ordinary ridge with one penalty parameter (Hastie and Tibshirani, 2004), which is useful for initializing the penalties. Then, we combine several matrix identities with a formulation of Iterative Weighted Least Squares (IWLS; used for GLM and Cox ridge regression) in terms of the linear predictors to allow an implementation with only one simple calculation in the high-dimensional feature space per data type: the product of the data matrix with its transpose. This calculation does not need to be repeated for folds of the CV, for different values of the penalties (proposed by the optimizer), or different sample weights in the IWLS algorithm. This renders `multiridge` very efficient for high-dimensional applications.

To broaden the application scope of `multiridge` we provide several extensions, including preferential ridge, which accounts for a preference for one data type over the other, and paired ridge, which shrinks parameters of paired covariates (e.g. the same gene measured on both DNA and mRNA). Other applications of the presented computational shortcuts are discussed as well, including kernel ridge regression and Bayesian probit ridge regression fit by a variational algorithm.

We supply details on the implementation, in particular on the optimization strategy used to find the best penalties. The computational gain of `multiridge` compared to more naive implementations is illustrated to be several orders of magnitude, which makes it useful as a standalone tool, but also as a fast benchmark for more complex multi-view models and (possibly sparse) learners. Several variations of `multiridge` are illustrated on four multi-omics TCGA data sets with survival response.

2 Contributions

Multi-penalty ridge is not new, and in fact already proposed by Hoerl and Kennard (1970). Our aim is to make the model practically usable for modern applications with multiple (very) high-dimensional data types, and linear, binary or survival response. We summarize the main contributions of this paper.

1. A computationally very efficient formula for the multi-penalty, sample-weighted hat-matrix, which is crucial in the IWLS algorithm for fitting GLM and Cox ridge regression
2. Extension to inclusion of non-penalized variables, essential in many clinical high-dimensional prediction problems to account for patient characteristics
3. Efficient CV which avoids repetitive computations in the high-dimensional space

4. Extension of the equality by Perrakis et al. (2019), here (10), to paired ridge (19)
5. R-software `multiridge` enabling multi-penalty ridge prediction and performance evaluation for a broad array of high-dimensional applications
6. Extension to Bayesian probit ridge regression with multiple penalties (prior precisions)

3 Fast CV for ordinary ridge

Efficient cross-validation for ridge with a single penalty parameter λ was discussed in Hastie and Tibshirani (2004). Let \mathbf{Y} be the linear response vector of length n (sample size), and X the $n \times p$ design matrix with p : the number of covariates. They show for the ridge estimator that:

$$\hat{\beta}_\lambda = (X^T X + \lambda I)^{-1} X^T \mathbf{Y} = V(R^T R + \lambda I)^{-1} R^T \mathbf{Y}, \quad (1)$$

where R and V are obtained by singular value decomposition (SVD) of X : $X = RV^T = UDV^T$. This hugely reduces computing time, as the second estimator requires inverting an $n \times n$ matrix instead of a $p \times p$ one. Importantly, they show that also for cross-validation as well as for GLM and Cox ridge regression only one SVD is required. The last equality in (1) breaks down, however, when λI is replaced by a diagonal matrix Λ with non-identical diagonal elements, as required for multi-penalty ridge. If one needs to evaluate only one value of Λ , this may be solved as in Van de Wiel et al. (2016) by an SVD on $X_\Lambda = X\Lambda^{-1/2}$. Repeating the SVD for many values of Λ is computationally costly, however, so therefore we develop an alternative approach. Nevertheless, fast CV for ordinary ridge will be useful to initialize multi-penalty ridge: simply cross-validate each data type separately, and use the obtained λ 's as starting values. Table 4 in the Appendix shows that the SVD-based CV implementation can be orders of magnitude faster than plain CV, in particular for large p . In all cases, the two methods rendered the exact same penalty. In case of leave-one-out CV the approximate method introduced by Meijer and Goeman (2013) can be competitive, in particular for large n and moderate p settings. However, when both n and p are large, SVD-based CV using a lower fold (e.g. 10) seems to be the only reasonable option.

4 Fast CV for multi-penalty ridge

Let X_b be the $n \times p_b$ design matrix representing the b th data type, $b = 1, \dots, B$. Then, the overall $n \times p, p = \sum_b p_b$, design matrix X is defined as:

$$X = [X_1 | X_2 | \dots | X_B].$$

Each X_b corresponds to a penalty λ_b . The optimal value of $\boldsymbol{\lambda} = (\lambda_b)_{b=1}^B$ will be determined by CV. Then, denote the penalty matrix by $\Lambda = \text{diag}(\lambda_1 \mathbf{1}_{p_1}, \lambda_2 \mathbf{1}_{p_2}, \dots, \lambda_B \mathbf{1}_{p_B})$, where $\mathbf{1}_{p_b}$ denotes a row vector of p_b 1's. The penalized log-likelihood equals

$$\ell^\Lambda(\boldsymbol{\beta}; \mathbf{Y}, X) = \ell(\boldsymbol{\beta}; \mathbf{Y}, X) - \frac{1}{2} \boldsymbol{\beta}^T \Lambda \boldsymbol{\beta} = \ell(\boldsymbol{\beta}; \mathbf{Y}, X) - \frac{1}{2} \sum_{b=1}^B \lambda_b \|\boldsymbol{\beta}_b\|_2^2, \quad (2)$$

where the factor 1/2 is used for convenience. This formulation is a special case of generalized ridge regression, already discussed by Hoerl and Kennard (1970). Firinguetti (1999) suggests

an estimator for Λ , but this only applies to low-dimensional linear models, as it relies on an initial OLS estimator. Our focus lies on efficient estimation of Λ by cross-validation in a generic, high-dimensional prediction setting. Therefore, our aim is to efficiently maximize the cross-validated likelihood (CVL; Van Houwelingen et al., 2006):

$$\hat{\Lambda} = \operatorname{argmax}_{\Lambda} \operatorname{CVL}(\Lambda; \mathbf{Y}, X), \quad (3)$$

where

$$\operatorname{CVL}(\Lambda; \mathbf{Y}, X) = \sum_{i=1}^n \ell(\hat{\boldsymbol{\beta}}_{(-i)}^{\Lambda}; Y_i, \mathbf{X}_{i.}),$$

with

$$\hat{\boldsymbol{\beta}}_{(-i)}^{\Lambda} = \operatorname{argmax}_{\boldsymbol{\beta}} \ell^{\Lambda}(\boldsymbol{\beta}; \mathbf{Y}_{-f(i)}, X_{-f(i)}),$$

and $-f(i)$ denoting removal of all samples in the same fold as sample i . Later, we discuss extensions to other performance criteria than CVL.

By definition, the CVL is fully determined by the linear predictor $\mathbf{X}_{i.}\hat{\boldsymbol{\beta}}_{(-i)}^{\Lambda}$ in GLM and Cox, which will be exploited throughout this manuscript. All estimates depend on Λ , so when cross-validating the number of evaluations of Λ can be huge: $n_{\Lambda} \cdot n_{\text{fold}} \cdot \bar{n}_W$, where n_{Λ} is the number of penalty parameter configurations that will be considered by the optimizer, n_{fold} is the number of folds, and \bar{n}_W is the average number of weight vectors the IWLS algorithm below requires to converge across all folds and Λ settings. Hence, each estimate needs to be computed very efficiently.

We fit a ridge-penalized GLM using an iterative weighted least squares (IWLS) algorithm, which is equivalent to Newton updating. Cox ridge regression is very similar in spirit (see Van Houwelingen et al. (2006); further details are supplied in the Appendix). Let $\boldsymbol{\eta}$ be the linear predictor, for example initialized by $\boldsymbol{\eta} = \mathbf{0}_n$, which we wish to update. The following steps are key to IWLS, here presented in the context of logistic ridge regression:

Algorithm 1 IWLS algorithm

Initialize $\boldsymbol{\eta}$.

Cycle:

$$\tilde{Y}_i \leftarrow \operatorname{expit}(\eta_i), \tilde{\mathbf{Y}} = (\tilde{Y}_i)_{i=1}^n \quad (\text{vectorized predictions}) \quad (4)$$

$$w_i \leftarrow \tilde{Y}_i(1 - \tilde{Y}_i), W = \operatorname{diag}((w_i)_{i=1}^n) \quad (\text{sample weights}) \quad (5)$$

$$\mathbf{C} \leftarrow \mathbf{Y} - \tilde{\mathbf{Y}} \quad (\text{centered response vector}) \quad (6)$$

$$H_{\Lambda, W} \leftarrow X(\Lambda + X^T W X)^{-1} X^T \quad (\text{hat matrix}) \quad (7)$$

$$\boldsymbol{\eta}_{\Lambda, W} \leftarrow H_{\Lambda, W}(\mathbf{C} + W\boldsymbol{\eta}), \boldsymbol{\eta} = \boldsymbol{\eta}_{\Lambda, W} \quad (\text{linear predictor update}) \quad (8)$$

Here, the updating for $\boldsymbol{\eta}$ follows from applying Newton's method (see Appendix). For other GLMs, one simply needs to replace \tilde{Y}_i and w_i by $E(Y_i|\eta_i)$ and $V(Y_i|\eta_i)$, respectively. Note that one may account for an offset by simply including it as $\tilde{\mathbf{Y}} = \operatorname{expit}(\boldsymbol{\eta}_0 + \boldsymbol{\eta})$. Moreover, note that for linear response \mathbf{Y} , no updating and weights are required, as we simply have $\boldsymbol{\eta} = H_{\Lambda, I_n} \mathbf{Y}$.

IWLS relies on iterative updating of these quantities until convergence. Note that the computation of $\boldsymbol{\eta}$ does *not* require the large parameter estimate vector $\hat{\boldsymbol{\beta}}_{\Lambda}$, but instead relies

crucially on the $n \times n$ hat matrix $H_{\Lambda, W}$. Below we show how to efficiently compute this. When we use CV to find Λ , many versions of $H_{\Lambda, W}$ need to be computed, because besides Λ and W , also the design matrix X varies due to CV. The derivations below show that all these instances of (W, Λ, X) together require to compute the B block-wise sample correlation matrices $S_b = X_b X_b^T$ *only once*. Then, this is the only computation in dimension of order p ; all other computations are in dimension n or lower. We start with the setting with all $\lambda_b > 0$, which we then extend to allow for an unpenalized block, $\lambda_0 = 0$. Finally, we show how to adapt the calculations in settings where the design matrix X changes, such as for CV and prediction for new samples.

4.1 All covariates penalized

Here, assume that all covariates are penalized, so $\forall b : \lambda_b > 0$. We set out to efficiently compute $H_{\Lambda, W} = X(\Lambda + X^T W X)^{-1} X^T$, for possibly many different values of W and Λ . We first apply Woodbury's identity to convert matrix inversion of the large $p \times p$ matrix to that of an $n \times n$ matrix plus some matrix multiplications:

$$(\Lambda + X^T W X)^{-1} = \Lambda^{-1} - \Lambda^{-1} X^T (W^{-1} + X \Lambda^{-1} X^T)^{-1} X \Lambda^{-1}. \quad (9)$$

The most costly operation in (9) is the matrix multiplication $X \Lambda^{-1} X^T$, as X has dimensions $n \times p$. As noted by Perrakis et al. (2019), we have

$$\Gamma_{\Lambda} = X \Lambda^{-1} X^T = \sum_{b=1}^B \lambda_b^{-1} \Sigma_b, \text{ with } \Sigma_b = X_b X_b^T. \quad (10)$$

This is computationally very useful, because it means that once the B $n \times n$ matrices Σ_b are computed and stored, $\Gamma_{\Lambda} = X \Lambda^{-1} X^T$ is quickly computed for any value of Λ . Finally, we have:

$$\begin{aligned} H_{\Lambda, W} &= X(\Lambda + X^T W X)^{-1} X^T \\ &= X \left(\Lambda^{-1} - \Lambda^{-1} X^T (W^{-1} + X \Lambda^{-1} X^T)^{-1} X \Lambda^{-1} \right) X^T \\ &= \Gamma_{\Lambda} - \Gamma_{\Lambda} (W^{-1} + \Gamma_{\Lambda})^{-1} \Gamma_{\Lambda}, \end{aligned} \quad (11)$$

in which all matrices are of dimension $n \times n$, and hence the matrix operations are generally fast. The new linear predictor $\boldsymbol{\eta} = \boldsymbol{\eta}_{\Lambda, W}$ then equals $H_{\Lambda, W}(C + W\boldsymbol{\eta})$, after which (4) to (8) are updated accordingly in the IWLS algorithm.

4.2 Including unpenalized covariates

Often it is desirable to include an intercept and also a few covariates without a penalty. E.g. in clinical genomics studies, patient information on age, gender, disease stage, etc. may be highly relevant for the prediction. In this setting, we need to augment Λ with zeros to obtain the entire penalty matrix Λ' . Then, (10) and (11) do not apply, because Λ'^{-1} is not defined when at least one of the diagonal elements equals 0. Replacing those by a small penalty may render the matrix calculations instable. Hence, we extended (11) to the setting which allows zero's on the diagonal of Λ' . First, define:

$$X \in \mathbb{R}^{n \times p}, X_1 \in \mathbb{R}^{n \times p_1}, X_2 \in \mathbb{R}^{n \times p_2}, \text{ s.t. } X = [X_1 | X_2],$$

and such that X_1 contains the covariates left unpenalized and X_2 the covariates to be penalized. Here, X_2 may consist of multiple blocks corresponding to penalty matrix Λ . Then, write the penalty matrix Λ' , which is rank deficient, as the two-by-two block matrix containing blocks of all zeros and a $p_2 \times p_2$ penalty matrix of full rank:

$$\Lambda' = \begin{bmatrix} \Lambda'_{11} & \Lambda'_{12} \\ \Lambda'_{21} & \Lambda'_{22} \end{bmatrix} = \begin{bmatrix} \mathbf{0}_{p_1 \times p_1} & \mathbf{0}_{p_1 \times p_2} \\ \mathbf{0}_{p_2 \times p_1} & \Lambda \end{bmatrix}. \quad (12)$$

Furthermore, assume that X_1 has linearly independent columns (in the algebraic sense), i.e. $\text{rank}(X_1) = p_1 \leq n$. Moreover, let $X_{k,W} = W^{1/2}X_k$, for $k = 1, 2$, and define the projector $P_{1,W} = I_{n \times n} - X_{1,W}(X_{1,W}^T X_{1,W})^{-1} X_{1,W}^T$. Write (7) as $H_{W,\Lambda} = X(X^T W X + \Lambda')^{-1} X^T = W^{-1/2} X_W (X_W^T X_W + \Lambda')^{-1} X_W^T W^{-1/2}$.

Proposition 1

$$H_{W,\Lambda} = W^{-1/2} X_{1,W} (X_{1,W}^T X_{1,W})^{-1} X_{1,W}^T \left(I_{n \times n} - W^{1/2} H_{2,W,\Lambda} W^{1/2} \right) W^{-1/2} + H_{2,W,\Lambda}, \quad (13)$$

with

$$H_{2,W,\Lambda} = W^{-1/2} \Gamma_{W,\Lambda} \left(I_{n \times n} - (I_{n \times n} + P_{1,W} \Gamma_{W,\Lambda})^{-1} P_{1,W} \Gamma_{W,\Lambda} \right) P_{1,W} W^{-1/2}, \quad (14)$$

where

$$\Gamma_{W,\Lambda} = W^{1/2} \left(\sum_{b=1}^B \lambda_b^{-1} \Sigma_{2,b} \right) W^{1/2} \quad (15)$$

and $\Sigma_{2,b}$ as in (10), with X_b replaced by $X_{2,b}$. The result is proven in the Appendix. Once $\Sigma_{2,b}$ is known for blocks $b = 1, \dots, B$ all operations in (14) and (15) are on matrices with dimensions n or smaller.

4.3 Prediction on new samples and final coefficients

The Appendix shows how to use the results above to perform predictions on new samples, and generate estimated coefficients $\hat{\beta}_\Lambda$. The latter does inevitably imply one more multiplication of a $p \times n$ and $n \times n$ matrix, but this needs to be executed only once for the optimal $\hat{\Lambda}$ and converged weights W .

4.4 Efficient CV

Use of the Woodbury identity, which replaces matrices of the form $X^T X$ by $X X^T$, has a secondary convenient consequence, apart from the much smaller matrices to invert: it allows for very efficient cross-validation. Computation of the CVL (3) requires the linear predictors for left-out samples. For that (7) and (8) can be used after replacing the first matrix X in (7) by $X_{\text{out}} = X[\text{out},]$, and the others by $X_{\text{in}} = X[\text{in},]$, where ‘out’ (‘in’) denotes the sample indices of the left-out (left-in) samples and $[\text{out},]$ (or $[\text{in},]$) selects the corresponding rows. Then, analogously to (11), we have

$$H_{W,\Lambda,\text{out}} = X_{\text{out}} (\Lambda + X_{\text{in}}^T W X_{\text{in}})^{-1} X_{\text{in}}^T = \Gamma_{\Lambda,\text{out},\text{in}} - \Gamma_{\Lambda,\text{out},\text{in}} (W^{-1} + \Gamma_{\Lambda,\text{in},\text{in}})^{-1} \Gamma_{\Lambda,\text{in},\text{in}}, \quad (16)$$

with $\Gamma_{\Lambda,\text{out},\text{in}} = X_{\text{out}} \Lambda^{-1} X_{\text{in}}^T = \sum_{b=1}^B \lambda_b^{-1} \Sigma_{b,\text{out},\text{in}}$ and $\Sigma_{b,\text{out},\text{in}} = X_b[\text{out},] (X_b[\text{in},])^T$. $\Gamma_{\Lambda,\text{in},\text{in}}$ and $\Sigma_{b,\text{in},\text{in}}$ are defined analogously, and these are also required within the IWLS algorithm,

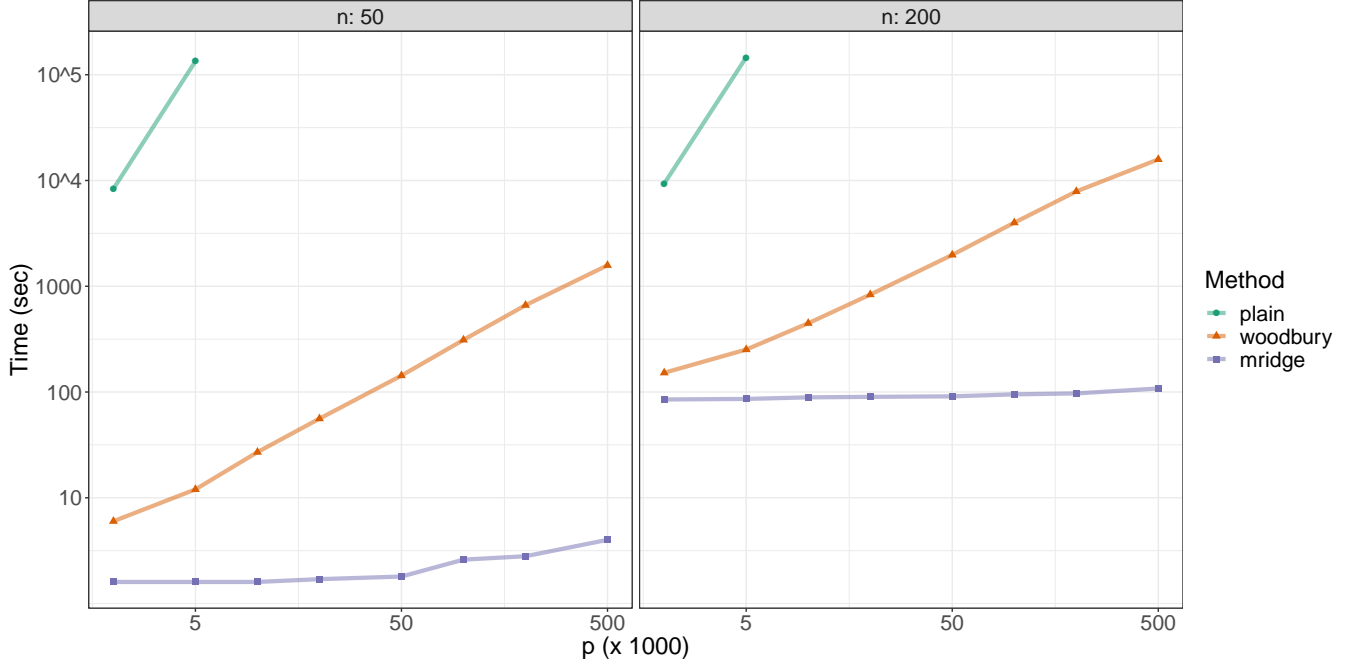


Figure 1: Computing times for 1000 evaluations of $(\Lambda, W, \text{Folds})$

as this is applied to the training (‘in’) samples. These matrices are conveniently obtained from $\Sigma_b = X_b X_b^T$, which is computed only once from the entire data set, because:

$$\Sigma_{b,\text{out},\text{in}} = \Sigma_b[\text{out}, \text{in}], \quad \Sigma_{b,\text{in},\text{in}} = \Sigma_b[\text{in}, \text{in}],$$

and therefore also:

$$\Gamma_{\Lambda,\text{out},\text{in}} = \Gamma_{\Lambda}[\text{out}, \text{in}], \quad \Gamma_{\Lambda,\text{in},\text{in}} = \Gamma_{\Lambda}[\text{in}, \text{in}]. \quad (17)$$

Likewise, this applies to the setting with an unpenalized data block for the computation of the cross-validation versions of $H_{2,W,\Lambda}$ (14) and $\Gamma_{W,\Lambda}$ (15).

5 Computing times for simulated cases

Figure 1 displays computing times on a PC with a 2.20GHz core for several simulated cases. We show results for $n = 50$ and $n = 200$, and varying p , where $p = 2 + 2 * p_{\text{pen}}$, with 2: the number of unpenalized covariates and p_{pen} : the size of each of the $B = 2$ penalized data blocks. We assume 1,000 evaluations of $(\Lambda, W, \text{folds})$. E.g. for K -fold CV with $K = 10$ and for an average number of IWLS iterations of 5, this implies evaluation of $1000/(5*10) = 20$ different values of Λ by the optimizer. This is still fairly modest, and for $B \geq 2$ often a larger number of Λ 's will be evaluated. The figure clearly shows the substantial computational benefit of **multiridge** w.r.t. to plain ridge fitting and ridge fitting with Woodbury's identity.

6 Implemented extensions

Below we present several extensions available in the software `multiridge`. Some of these will be illustrated for the data applications.

6.1 Extension 1: Repeated CV

To increase stability, some have argued for *repeated* CV to optimize the penalty parameters (Boulesteix et al., 2017). A theoretical argument for repetition of subsampling is found in Fong and Holmes (2019), who establish an equivalence with marginal likelihood optimization. Our software allows repeated CV. Computing time is linear in the number of repeats, so for this the computational shortcuts presented here should be very useful. In the linear case with Gaussian error, the marginal likelihood is analytical, which provides an alternative for estimating Λ (Veerman et al., 2020). Optimization of the marginal likelihood requires (multiple) evaluations of covariance matrix $\sigma I_n + X\Lambda^{-1}X^T$, which also benefits from the use of (10) (Perrakis et al., 2019).

6.2 Extension 2: Alternative CV criteria

We generally recommend to use cross-validated (partial) likelihood as the utility criterion for maximizing $\Lambda = \text{diag}(\boldsymbol{\lambda})$, as this is consistent with the likelihood criterion used to fit the model, given Λ . Moreover, it is a smooth function, which benefits optimization algorithms, unlike ranking-based alternatives like area-under-the-roc-curve (AUC). Nevertheless, in some cases one may want to explicitly maximize an alternative criterion, e.g. because it is better interpretable than CVL, or matches with the criterion used to evaluate and compare the predictors with alternative ones. Our software allows the user to supply a user-specific utility function, to be combined with any of the optimizers available in R’s `optim` function. Generally, for non-smooth utilities like AUC, optimizers require more evaluations of the objective function than for smooth ones, and may converge to a local optimum. The latter problem can be alleviated by repeated CV, although the resulting profile is likely flatter than that of CVL (see Appendix Figure 5), which may cause the optimizer to terminate too early. In any case, the larger number of evaluations required by alternative, non-smooth utility criteria warrants the usefulness of the computational shortcuts presented here.

6.3 Extension 3: Paired ridge

For some applications, the variables in X are paired, and one may want to make use of this information by coupling the corresponding parameters. A well-known example are genes measured on mRNA and DNA for the same samples, in which case one may want to couple parameters corresponding to the same gene. Another example is two transformations or representations of the same data, e.g. continuous gene expression and binarized gene expression, low versus high. We assume paired columns are juxtaposed in X : $X = (\mathbf{X}_{1,.1}, \mathbf{X}_{2,.1}, \mathbf{X}_{1,.2}, \mathbf{X}_{2,.2}, \dots, \mathbf{X}_{1,.p}, \mathbf{X}_{2,.p})$, where $\mathbf{X}_{k,.j}$ denotes the j th column of one of the two design matrices X_k . Then, the first equality for the penalized likelihood in (2) still holds, but Λ is now a block diagonal matrix:

$$\Lambda = I_p \otimes \Lambda_s = I_p \otimes \begin{bmatrix} \lambda_1 & -\lambda_3 \\ -\lambda_3 & \lambda_2 \end{bmatrix},$$

because for two paired parameters (β_j, β'_j) one wishes to employ a penalty

$$\tilde{\lambda}_1 \beta_j^2 + \tilde{\lambda}_2 (\beta'_j)^2 + \tilde{\lambda}_c (\beta_j - \beta'_j)^2 = \lambda_1 \beta_j^2 + \lambda_2 (\beta'_j)^2 - \lambda_3 \beta_j \beta'_j, \quad (18)$$

with $\lambda_1 = \tilde{\lambda}_1 + \tilde{\lambda}_c, \lambda_2 = \tilde{\lambda}_2 + \tilde{\lambda}_c, \lambda_3 = \tilde{\lambda}_c$. An alternative formulation for the paired penalty is $\tilde{\lambda}_c (\tilde{\lambda}_1^{1/2} \beta_j - \tilde{\lambda}_2^{1/2} \beta'_j)^2$, which scales the β 's with their prior standard deviations, i.e. $1/\tilde{\lambda}_k^{1/2}, k = 1, 2$, rendering the pairing possibly more natural. The two formulations, however, are equivalent, as one obtains the right-hand side of (18) by setting $\lambda_1 = \tilde{\lambda}_1(1 + \tilde{\lambda}_c), \lambda_2 = \tilde{\lambda}_2(1 + \tilde{\lambda}_c), \lambda_3 = (\tilde{\lambda}_1 \tilde{\lambda}_2)^{1/2} \tilde{\lambda}_c$. Note that the latter equivalence is useful for initialization: suppose that for $k = 1, 2$, $\tilde{\lambda}_k$ has been determined by fast uni-penalty CV, and one initializes $0 < \tilde{\lambda}_c < 1$ as the relative paired penalty (e.g. $\tilde{\lambda}_c = 1/4$), then the implied initial values of $(\lambda_1, \lambda_2, \lambda_3)$ should be roughly on the correct scale.

In this paired setting, we conveniently have $\Lambda^{-1} = I_p \otimes \Lambda_s^{-1} =: \Omega$. Write

$$\Omega_s = \Lambda_s^{-1} = \begin{bmatrix} \omega_1 & \omega_3 \\ \omega_3 & \omega_2 \end{bmatrix}.$$

Then,

$$\Gamma_\Lambda = X \Lambda^{-1} X^T = X \Omega X^T = \omega_1 X_1 X_1^T + \omega_2 X_2 X_2^T + \omega_3 X Q X^T, \quad Q = I_p \otimes \begin{bmatrix} 0 & 1 \\ 1 & 0 \end{bmatrix}. \quad (19)$$

Therefore, also in this setting computations are very efficient once the $n \times n$ matrices $\Sigma_k = X_k X_k^T, k = 1, 2$ and $\Sigma_Q = X Q X^T$ are computed and stored. Here, Q is a large $2p \times 2p$ matrix, but does not need to be generated for computing Σ_X : Q is a permutation matrix, so XQ is simply computed by swapping the paired columns in X . These results trivially extend to triplets or larger blocks of variables. As long as these blocks are small, inversion of Λ is fast and so is the computation of Γ_Λ . It also extends easily to combinations with block(s) of unpaired variables: simply apply (19) to the paired variables and add this to (10), which is applied to the unpaired variables.

With a small modification, the above also applies to settings where X_1 and X_2 are measured on *different* individuals, and one still wishes to couple paired parameters. For example, when two studies have a similar (but not the same) set-up and measure the same, or very similar features, such as normalized mRNA gene expression measured by microarray and RNAseq technology. Simply create X by juxtaposing columns $\mathbf{X}_{1,j}^0 = (X_{1,1j}, \dots, X_{1,n_1j}, \mathbf{0}_{n_2})^T$ and $\mathbf{X}_{2,j}^0 = (\mathbf{0}_{n_1}, X_{2,1j}, \dots, X_{2,n_2j})^T$, so 0s are inserted for individuals for which either X_1 or X_2 does not apply. Then, the two covariate sets correspond to two different parameter estimates, but these are shrunken towards one another.

Finally, note that fusing is another mechanism to couple parameters, e.g. when an ordering is known, such as DNA position of a gene (Chaturvedi et al., 2014). This leads to a banded Λ matrix. Efficient algorithms exist to compute the inverse of such matrices, which, however, is generally dense. The latter precludes efficient (repeated) computation of $\Gamma_\Lambda = X \Lambda^{-1} X^T$.

6.4 Extension 4: Preferential ridge

Sometimes, one or more particular data types may be preferable over others, in particular when one believes that these data types generalize better to other settings. A well-known example in genomics is the preference for DNA-based markers (copy number, mutations,

methylation) over mRNA-based ones (gene expression). In an elastic net setting, a two-stage approach was proposed (Aben et al., 2016): first, an elastic net with the preferred markers was fitted, then the corresponding linear predictors were fixed as offsets, and the non-preferred (gene expression) markers were added using a second elastic net with those offsets. The authors show that such a strategy can perform competitively to the baseline strategy without preferential markers, while arguing that the two-stage model is likely more robust. The competitive performance was also observed by Klau et al. (2018), who employ a similar approach using a multi-stage lasso.

One could follow the same two-stage regression fitting in a ridge setting. The main strength of ridge regression, however, is that it deals well with collinearity among covariates. Also between data types such collinearity may be rather strong (e.g. DNA copy number and mRNA expression of the same gene can be strongly correlated in tumor profiles). This would be ignored when fitting the regression in two stages. Therefore, we prefer to fit one ridge regression in the end, but reflect the preference by first estimating $\boldsymbol{\lambda}$ using only the preferential data types, $\mathcal{P} \subset \{1, \dots, B\}$. Then, the corresponding penalties, $\boldsymbol{\lambda}_{\mathcal{P}} = (\lambda_b)_{b \in \mathcal{P}}$, are fixed, and $\boldsymbol{\lambda}_{\mathcal{P}^c} = (\lambda_b)_{b \notin \mathcal{P}}$ is optimized conditional on $\boldsymbol{\lambda}_{\mathcal{P}}$ using all covariates in the regression. We give a data example of this strategy below.

7 Software notes

7.1 Implementation, data and scripts

The method is implemented in R-package `multiridge`, available at <https://github.com/markvdwiel/multiridge>, which also links to a demo R-script. The demo includes the processed multi-omics TCGA data with survival response, discussed below. In addition, it includes a classification example on diagnostics of a pre-stage of cervical cancer using $p_1 = 699$ miRNAs and $p_2 \approx 365,620$ methylation markers. This demonstrates the computational efficiency of `multiridge` for large p . Further details and references on the data are supplied in the Appendix. To accommodate performance assessment on data, `multiridge` contains a function to perform double CV, which adds another loop of computations to the problem.

7.2 Checks

Results for estimating $\boldsymbol{\beta}$ (and hence $\boldsymbol{\eta} = X\boldsymbol{\beta}$) have been checked for correctness against the plain (but computationally inefficient) generalized ridge estimator for the linear regression case, $\hat{\boldsymbol{\beta}}_{\Lambda} = (X^T X + \Lambda)^{-1} X^T \mathbf{Y}$. These checks are also available as part of the code.

7.3 Optimization

We use R’s `optim` function to optimize CVL (3) w.r.t. $\boldsymbol{\lambda}$, the unique diagonal elements of Λ . The aforementioned SVD-based uni-penalty CV is used to initialize all B components of $\boldsymbol{\lambda}$. Our default optimization strategy after initialization is to first search globally by running a simulated annealer (SANN) using a limited number of iterations, e.g. 10. Then, we apply a more local method, defaulting to `Nelder-Mead` for multi-penalty optimization and `Brent` for uni-penalty optimization. In our experience, this strategy is robust against potential local optima, while still computationally efficient.

7.4 Parallel computing

The algorithm is parallelized at the level of the folds by distributing the computation of the contribution of each fold to the cross-validated likelihood (3) for given Λ . Note that the parallelization is very efficient, because (17) implies that the largest object to be distributed across nodes is the $n \times n$ matrix Γ_Λ .

8 Application: survival prediction with TCGA data

We use `multiridge` to predict overall survival from multi-omics TCGA data: microRNA expression (miRNA), messenger RNA gene expression (mRNA), and DNA copy number variation (CNV). Four tumor types were studied: Mesothelioma (MESO; $n = 84$), Kidney renal clear cell carcinoma (KIRC; $n = 506$), Sarcoma (SARC; $n = 253$) and Thymoma (THYM; $n = 118$). These four were chosen for their variability in sample size (but all larger than $n > 80$), availability of matched miRNA, mRNA and CNV data, and for showing some signal. Other (large) sets such as breast cancer and ovarian cancer (BRAC and OV) rendered no or a weak signal at best (c -index < 0.6) for any of the methods below, and hence these results were not shown. The data were preprocessed as described in Rauschenberger et al. (2019). Further details on the data are given in the Appendix.

The purpose of these analyses is three-fold: i) to report computing times for `multiridge` on real data with variable sample sizes; ii) to compare standard `multiridge` with preferential ridge (`multiridge_pref`), as well as with elastic net based benchmarks; and iii) to illustrate paired ridge (`multiridge_pair`) for a particular setting, and compare it with `multiridge`.

In all studies, we used $2/3^{\text{rd}}$ of the samples for training, and the remaining $1/3^{\text{rd}}$ for testing. The splitting was balanced in terms of the events (deaths). This was repeated thrice such that each sample was used once as a test sample. The training involved 10-fold cross-validation for determining the penalty parameters.

8.1 Application of preferential ridge and its benchmarks

For preferential ridge, we used miRNA and CNV as preferred data types and mRNA gene expression as secondary one. The first two are generally preferred in clinical practice for their better stability and robustness. As benchmarks we applied two variations of TANDEM (Aben et al., 2016), which is only implemented for linear regression. TANDEM uses a two-stage elastic net (EN), where the second stage fits the non-preferred markers to the residuals of the elastic net fitted to the preferred markers. Equivalently (in the linear setting), we introduce the n linear predictors of the first stage as offsets for the second stage elastic net. Advantage of this approach is that it can also be applied to GLM and Cox regression, which we need here. The first variation (EN2) uses miRNA and CNV together in the first stage, and mRNA in the second stage. The second variation (EN3) is a three-stage approach, using the order CNV \rightarrow miRNA \rightarrow mRNA, which, unlike EN2, allows different penalties for miRNA and CNV. We use `glmnet` to fit the elastic nets with defaults as in TANDEM ($\alpha = 0.5$ and $\lambda_1 = \text{lambda.1se}$).

8.2 Computing times

Table 1 shows computing times for `multiridge` and `multiridge_pref` using four nodes on a Windows x64 server, build 14393. The computing times were averaged over the three

data splits. Variation was small, hence not shown. We distinguish the computing times for initialization (using the efficient SVD-based CV for each omics-type separately) from those of the two multi-penalty approaches. For the latter two, the maximum number of optimization iterations was set to 10 and 25 for the global and local search by **SANN** and **Nelder-Mead/Brent**, respectively. We observe that computing times are very reasonable, even for the largest sample size, $n_{\text{train}} = 337$. Note that for linear models computing times should be substantially shorter as no IWLS iterations are needed; in addition, we noticed that logistic ridge is often faster than Cox ridge, as it tends to require fewer IWLS iterations. Finally, as a side note: the elastic net approaches fitted by **glmnet** (including CV of the penalty) roughly took 1.5-3 times more computing time, without parallel computation however.

8.3 Comparative performance

Figure 2 shows the comparative performances of **multiridge**, **multiridge_pref**, **EN2**, **EN3**, as evaluated on the three test sets by the c-index. Alternatively, we used cross-validated log-likelihood as evaluation criterion. This rendered qualitatively similar results, so these are not shown. First, we corroborate the results in (Aben et al., 2016) that the preferential approach (here, **multiridge_pref**) can indeed render very competitive results to the standard, non-preferential approach (**multiridge**). Second, we observe markedly better performance for the ridge-based methods than for the EN models for three out of four tumor types. We should, however, put this in perspective: the EN models have the advantage of selecting variables; therefore, for the KIRC data set, the EN models are likely preferable. For the THYM data set, performances vary substantially between splits due to the small number of events (9). Finally, Table 2 shows that preferential ridge (**multiridge_pref**) generally penalizes miRNA less than **multiridge** does, while penalizing the non-preferred marker, mRNA gene expression, much more. This leads to substantially larger (smaller) regression coefficients for miRNAs (mRNA) for **multiridge_pref**, as shown in Table 3.

	n_{train}	Init	multiridge	multiridge_pref
MESO	56	2.23	5.93	9.42
KIRC	337	87.14	102.30	143.56
SARC	168	14.65	14.81	24.02
THYM	78	2.58	7.76	15.73

Table 1: Computing times (sec) for initialization, **multiridge** and **multiridge_pref**

	multiridge			multiridge_pref		
	miRNA	mRNA	CNV	miRNA	mRNA	CNV
MESO	2103	8840	34068	394	15521	81201
KIRC	1334	44512	105079	834	64291	1.7e+6
SARC	4048	16472	13036	2254	20359	13398
THYM	47	14631	19376	73	2.2e+9	58108

Table 2: Median penalties (across three splits) per data set and type

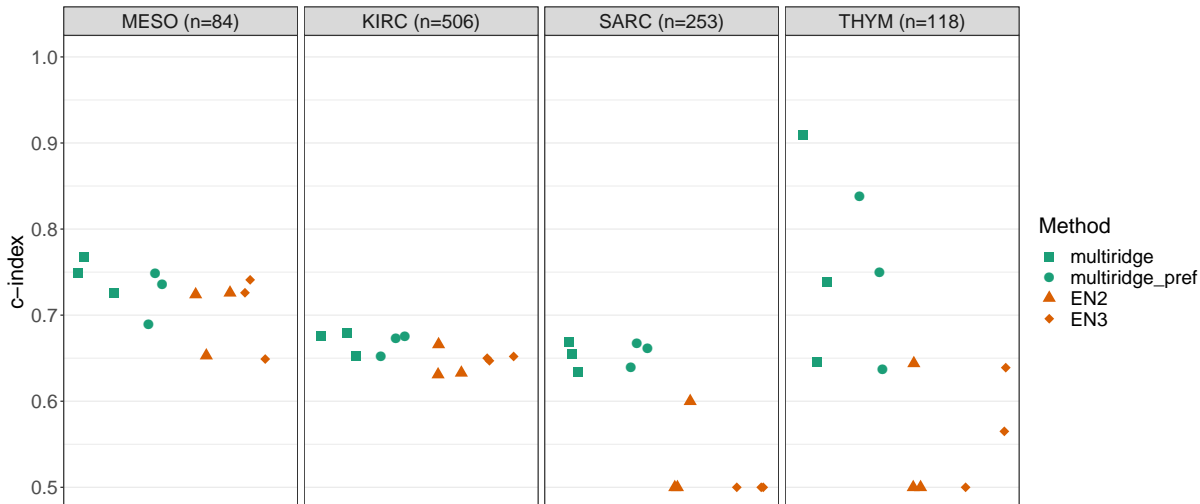


Figure 2: Predictive performance for three splits per data set, as measured by c-index (y-axis)

	multiridge			multiridge_pref		
	miRNA	mRNA	CNV	miRNA	mRNA	CNV
MESO	1.67	5.52	0.65	7.41	2.82	0.22
KIRC	6.17	2.49	0.36	8.88	1.85	0.03
SARC	1.57	4.45	3.06	2.73	3.62	2.97
THYM	10.21	0.48	0.13	9.98	0.00	0.05

Table 3: Median (across 3 splits) sum of absolute coefficients ($||\beta||_1$) per data set and type

8.4 Application of paired multiridge

As in ordinary regression settings, the best scale to represent a given data type is not known beforehand. In fact, in an adaptive elastic net setting, the joint use of a continuous and binary representation was shown to be potentially beneficial (Rauschenberger et al., 2019) for omics-based tumor classification. Our default multi-ridge (`multiridge`) allows for including both representations using different penalties to reflect different predictive signal for the two representations. In addition, paired multi-ridge (`multiridge_pair`) specifically accounts for the pairing by the paired penalty (18).

Using the MESO and KIRC mRNA gene expression data as presented above, we assessed whether augmenting this data with its binarized counterpart improved prediction of survival using the same 3-fold training-test setting as above. We simply binarized the gene expression data by using the median per gene as threshold. Low expression was represented by ‘-1’, high expression by ‘1’, implying that the binary data is on the same scale its continuous counterpart. Less than 10% of genes did not show any variation on the binary scale (genes with many zero counts), and were therefore filtered out. We noted that computing times were very similar to those in the first two rows of Table 1, and hence these are not further detailed here. Figure 3 shows the predictive performances for i) ordinary `ridge` using the continuous gene expression data only; ii) `multiridge` on both data representations with two unpaired penalties; and iii) `multiridge_pair` with an additional paired penalty. We observe

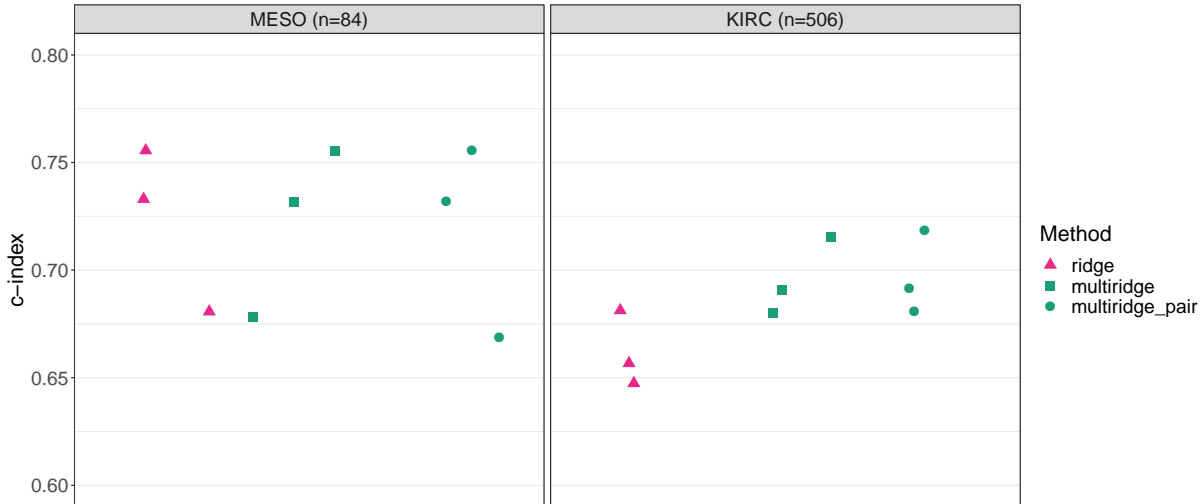


Figure 3: Predictive performance for three splits per data set, as measured by c-index (y-axis)

that performances are very much on par for the MESO data, whereas for the large KIRC set adding the binarized representation improves prediction. Pairing does not further improve the predictive performance here. Figure 4, however, shows that `multiridge_pair` has an edge in terms of interpretation: the paired penalty clearly increases the agreement between the two parameter estimates corresponding to the same gene. The figure shows the estimates for the first training-test split; results for other splits were very similar. Correlations between estimates averaged across splits are: 0.72 (0.90) for the MESO data and 0.58 (0.71) for the KIRC data using `multiridge` (`multiridge_pair`), again with very limited variability across splits. Chaturvedi et al. (2014) come to a similar conclusion for the fused lasso, which fuses parameters of neighboring genes on the genome: no or little improvement for prediction, but better interpretability due to increased agreement for estimates of neighboring genes.

9 Further extensions

We outline two extensions of the proposed method that are not part of `multiridge`.

9.1 Kernel ridge regression

Kernel ridge is a well-known extension to ordinary ridge regression in machine learning. In our setting, (10) shows that multi-penalty ridge predictions depend on the data-type $b = 1, \dots, B$ only via the scaled $n \times n$ sample covariance matrices $\Sigma_b = X_b X_b^T$. One may replace Σ_b by $\Sigma_b^K = K(X_b, X_b^T)$, where K is a kernel. Here, the inner product is referred to as the linear kernel. A consequence of the decomposition (10) is that different kernels may be used for different data-types, at no or little additional computational cost. In particular, a linear kernel may not be optimal for potentially unbalanced binary data types (such as mutational status). E.g. when using a conventional $(0, 1)$ coding we have $0 \cdot 0 = 0 \cdot 1 = 0$. That is, according to the linear kernel, the 5-feature mutational profile $[00000]$ is as close to $[11111]$ as it is to $[00000]$. Note that while an alternative binary coding like $(-1, 1)$ solves this issue, it

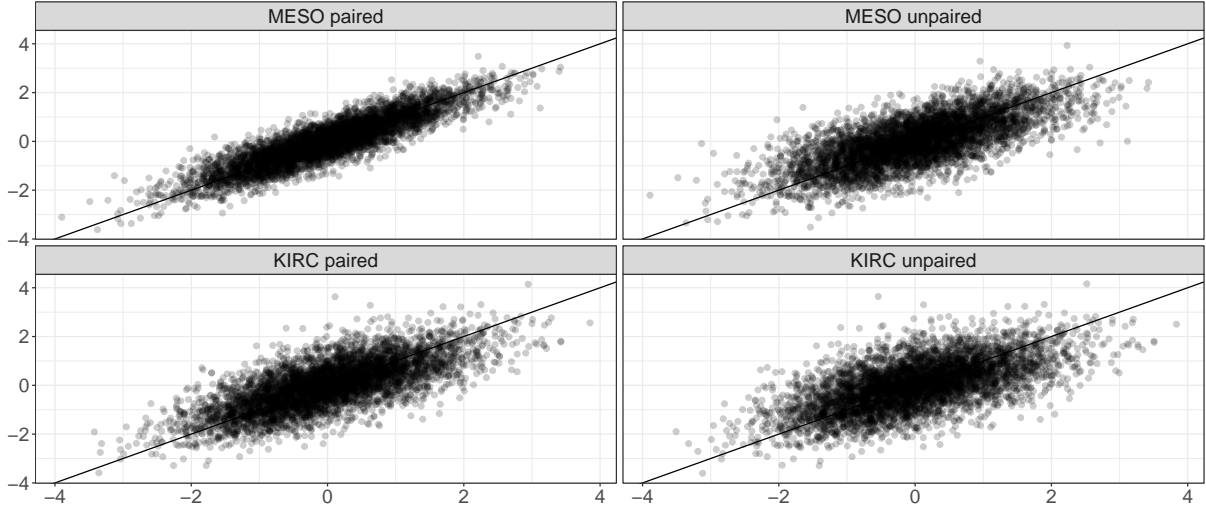


Figure 4: Standardized estimated β 's for the continuous (x-axis) and binarized (y-axis) expression values

leads to another one: it would value an agreement between samples on occurrence of the (say rare) event (denoted by a '1', like a mutation) as much as agreement of the non-occurrence (-1). For potentially better agreement measures one may either turn to well-known statistical measures as Cohen's kappa or the Jaccard index. Alternatively, one may try to learn a kernel, preferably in a semi-supervised framework to make use of large numbers of unlabeled observations (Salakhutdinov and Hinton, 2008). Note that while non-linear kernels can be used in our framework to produce predictions, they do not (easily) allow interpretation on the covariate level, because the translation to coefficients (β) is lost.

9.2 Bayesian multi-penalty probit ridge regression

The reparametrization $\beta \rightarrow \eta$ to gain computational efficiency applies to other versions of multi-penalty ridge regression as well. For the linear case, Perrakis et al. (2019) use equality (10) to derive very efficient algorithms for obtaining posteriors from Bayesian multi-penalty ridge regression. Here, we extend this to Bayesian probit ridge regression for handling binary response by reformulating the variational Bayes (VB) algorithm in (Ormerod and Wand, 2010). An auxiliary variable is introduced to make VB steps tractable. The model with binary response $\mathbf{Y} \in \mathbb{R}^n$, auxiliary variable $\mathbf{a} \in \mathbb{R}^n$, observed data $X \in \mathbb{R}^{n \times p}$ and regression coefficients $\beta \in \mathbb{R}^p$ is given by:

$$\begin{aligned}
 y_i | a_i &\stackrel{ind.}{\sim} \pi(y_i | a_i) = I(a_i \geq 0)^y I(a_i < 0)^{1-y_i} \\
 a_i | \beta &\stackrel{ind.}{\sim} N((X\beta)_i, 1) \\
 \beta | \mu_\beta, \Sigma_\beta &\sim N(\mu_\beta, \Sigma_\beta).
 \end{aligned}$$

We consider prior mean $\mu_\beta = \mathbf{0}$ and $\Sigma_\beta = \Lambda^{-1}$, as in the multi-penalty ridge regression.

The posterior q is approximated under the assumption that the posterior factorizes over \mathbf{a} and β : $q(\mathbf{a}, \beta) = q_a(\mathbf{a})q_\beta(\beta)$. The VB estimates q_a^*, q_β^* are then analytical and are found by

iteratively updating the posterior means of \mathbf{a} and $\boldsymbol{\beta}$, denoted by $\boldsymbol{\mu}_{q(\mathbf{a})}$ and $\boldsymbol{\mu}_{q(\boldsymbol{\beta})}$ (Ormerod and Wand, 2010, Algorithm 4). As the update for $\boldsymbol{\mu}_{q(\mathbf{a})}$ only depends on $\boldsymbol{\mu}_{q(\boldsymbol{\beta})}$ via $\boldsymbol{\mu}_{q(\boldsymbol{\eta})} = X\boldsymbol{\mu}_{q(\boldsymbol{\beta})}$, the iterative steps in their Algorithm 4 can be conveniently rewritten in lower-dimensional computations. Recall that the hat-matrix $H_\Lambda = H_{\Lambda, I_n} = X(X^T X + \Lambda)^{-1} X^T$ is efficiently computed using (10) and (11). Algorithm 4 in (Ormerod and Wand, 2010) is then restated in the n -dimensional (hence low-dimensional) space in Algorithm 2. Note the similarities of

Algorithm 2 VB scheme to approximate posteriors for Bayesian probit ridge regression in n -dimensional space

Initialize $\boldsymbol{\mu}_{q(\mathbf{a})}$.

Cycle:

$$\begin{aligned} \boldsymbol{\mu}_{q(\boldsymbol{\eta})} &\leftarrow X(X^T X + \Lambda)^{-1} X^T \boldsymbol{\mu}_{q(\mathbf{a})} = H_\Lambda \boldsymbol{\mu}_{q(\mathbf{a})} \\ \boldsymbol{\mu}_{q(\mathbf{a})} &\leftarrow \boldsymbol{\mu}_{q(\boldsymbol{\eta})} + \frac{\phi(\boldsymbol{\mu}_{q(\boldsymbol{\eta})})}{\Phi(\boldsymbol{\mu}_{q(\boldsymbol{\eta})})^{\mathbf{Y}} (\Phi(\boldsymbol{\mu}_{q(\boldsymbol{\eta})}) - \mathbf{1}_n)^{\mathbf{1}_n - \mathbf{Y}}}, \end{aligned}$$

where Φ denotes the standard normal CDF.

Algorithm 2 with the IWLS algorithm: an auxiliary variable is used to ‘linearize’ the response (W for IWLS), and alternating updating is required. VB algorithms use a lower bound of the marginal likelihood, the evidence lower-bound (elbo) to monitor convergence. In addition, analogously to CVL in the frequentist approach, the elbo may be used as a maximization criterion to estimate hyperparameters, here Λ , rendering a variational Bayes-empirical Bayes algorithm (Van de Wiel et al., 2018). Ormerod and Wand (2010) present an expression for the elbo in terms of $\boldsymbol{\beta}$. Some algebra (see Appendix) shows that the elbo can also be entirely expressed in terms of (the current estimates of) $\boldsymbol{\mu}_{q(\boldsymbol{\eta})}$, $\boldsymbol{\mu}_{q(\mathbf{a})}$, H_Λ and Γ_Λ , which are efficiently computed for multiple Λ s using (10) and (11). This facilitates fast optimization of the elbo in terms of Λ .

Once Λ is fixed, Algorithm 2 produces predictions $\boldsymbol{\mu}_{q(\boldsymbol{\eta})}$ and their uncertainties: the approximate posterior of $\boldsymbol{\eta} = X\boldsymbol{\beta}$ is $N(\boldsymbol{\mu}_{q(\boldsymbol{\eta})}, H_\Lambda)$, which follows from the expression for the posterior of $\boldsymbol{\beta}$ (Ormerod and Wand, 2010). Predictions and uncertainties on the probabilistic scale, $\Phi(\boldsymbol{\eta})$, follow straightforwardly.

Finally, to use Algorithm 2 in practice a Bayesian evaluation of predictive performance is required. Given that the elbo is an approximate likelihood in terms of the hyperparameters, it can not be used to compare models with a different number of hyperparameters, e.g. corresponding to a different number of data types in our setting. Instead, we propose using the Bayesian counterpart of CVL, the conditional predictive ordinate (CPO), which is the geometric mean of $\pi(Y_i | \mathbf{Y}_{-i})$: the likelihood of Y_i given (a model trained on) \mathbf{Y}_{-i} , where ‘training’ includes hyperparameter optimization. As we show in the Appendix, the CPO can also be expressed in terms of $\boldsymbol{\eta}$, and only requires computing n one-dimensional integrals. This facilitates fast Bayesian performance evaluation.

10 Discussion

Multi-penalty ridge is a multi-view penalized method. Several other methods estimate multiple penalty parameters in penalized regression. For sparse settings, Boulesteix et al. (2017) introduced `IPF-lasso`, which cross-validates all penalties in a lasso setting. As one often does not know whether a sparse or dense setting applies, a reasonable strategy in practice may be

to apply both methods to the data at hand, and compare the predictive performances. If a small predictive model is desirable, post-hoc variable selection may be applied to the ridge model (Bondell and Reich, 2012). Alternatively, (empirical) Bayes methods for estimating hyperparameters are available for ridge (Van de Wiel et al., 2016, **GRridge**), the elastic net (Münch et al., 2019, **gren**) and spike-and-slab models (Velten and Huber, 2018, **graper**). These methods adaptively estimate hyperparameters for possibly many groups of variables. When developing and testing **GRridge**, however, we noticed that empirical Bayes estimation of the penalties was inferior to CV when applied to groups that represent different data types, in particular when dimensions differ substantially. The two ridge-based methods should, however, integrate well. Hence, a future research direction is to merge multi-penalty estimation across (**multiridge**) and within (**GRridge**) data types.

Multi-view or integrated learners are not necessarily better than learners that use one single data type, in particular when assessed on one’s own data. In clinical genomics, it is often difficult to improve RNA-based predictions by adding other genomic data types (Aben et al., 2016). Broët et al. (2009) showed, however, that integrating DNA-based markers with RNA-based ones lead to a more robust classifier with a lower generalization error. This was also a reason to allow a preference for particular data type(s) in **multiridge**.

We focused on high-dimensional prediction for clinical studies, in which sample sizes are usually small to modest at most. For large n applications, say several thousands or more, other algorithms than IWLS, such as stochastic gradient descent, may be more efficient. Whether and how this applies to our setting, including unpenalized covariates, non-linear and possibly censored response and the estimation of multiple penalties, is left as a future research direction.

Our computational shortcuts apply also to Bayesian counterparts of multi-penalty ridge regression. For probit ridge regression we developed an n -dimensional version of a variational algorithm by Ormerod and Wand (2010), and showed how to efficiently estimate the penalties by expressing the lower bound for the marginal likelihood in terms of the hat-matrix. The results is an efficient Bayesian multi-view classifier for high-dimensional data. It complements **multiridge**, with the additional benefit of providing uncertainties of parameters and predictions.

We realize that **multiridge** is based on a simple, one-layer model. Hence, more advanced models may certainly outperform **multiridge** for data that supports sparse, non-linear, or multi-layer representations. This often comes at the price of reduced interpretation, and sometimes also with (partly) subjective hyperparameter tuning, which may lead to inferior generalization. In any case, a quick comparison with **multiridge** allows one to judge whether the margin in terms of performance counterbalances the differences in complexity, interpretation, and level of subjectivity. To conclude, we believe the use of **multiridge** is two-fold: first, for users as a versatile, interpretable stand-alone multi-view learner; and second, for developers as a fast benchmark for more advanced, possibly sparse, models and multi-view learners.

11 Appendix: Computing times CV single penalty ridge

Below we present computing times for plain CV, fast CV using SVD, and approximated leave-one-out CV (LOOCV) as discussed in (Meijer and Goeman, 2013). Table 4 presents results for LOOCV and 10-fold CV. Data sets used are: 1) the methylation data set **dataFarkas**

as available in the R-package **GRRidge** (Van de Wiel et al., 2016), which has dimensions $n \times p = 37 \times 40,000$ and binary response; 2) the MESO miRNA data set presented in the main document, with dimensions $84 \times 1,398$ and survival response; 3) as 2) but mRNA, with dimensions $84 \times 19,252$; 4) the KIRC miRNA data set presented in the main document, with dimensions $506 \times 1,487$ and survival response; 5) as 4) but mRNA, with dimensions $506 \times 19,431$.

data set	Dimensions		LOOCV			10-fold	
	n	$p(\times 1,000)$	Plain	SVD	Approx	Plain	SVD
1	37	40.0	46.96	1.81	12.09	20.35	0.77
2	84	1.4	26.75	13.46	3.98	4.35	1.95
3	84	19.3	200.08	13.27	23.12	31.04	2.22
4	506	1.5	>2,000	>2,000	85.47	154.78	112.97
5	506	19.4	>2,000	>2,000	>2,000	1,713.50	146.62

Table 4: Computing times in seconds

12 Appendix: Updating linear predictor

The IWLS updating for $\beta = (\beta_j)_{j=1,\dots,p}$ is well-known to be equivalent to Newton updating:

$$\beta^{\text{new}} = \beta - \mathbf{H}^{-1} \mathbf{g},$$

where \mathbf{H} and \mathbf{g} are the Hessian and gradient function of the objective function (here penalized log-likelihood), respectively. Therefore,

$$\eta^{\text{new}} = \eta - X\mathbf{H}^{-1}\mathbf{g}.$$

We have

$$\begin{aligned} \mathbf{H} &= -X^T W X - \Lambda, \\ \mathbf{g} &= X^T \mathbf{C} - \Lambda \beta, \end{aligned} \tag{20}$$

with $\mathbf{C} = \mathbf{Y} - \tilde{\mathbf{Y}}$, i.e. the response centered around the current prediction. Substitution renders

$$\begin{aligned} \eta^{\text{new}} &= \eta + X(X^T W X + \Lambda)^{-1} X^T \mathbf{C} - X(X^T W X + \Lambda)^{-1} \Lambda \beta \\ &= H_{\Lambda, W} \mathbf{C} + X(\beta - (X^T W X + \Lambda)^{-1} \Lambda \beta) \\ &= H_{\Lambda, W} \mathbf{C} + X(X^T W X + \Lambda)^{-1} ((X^T W X + \Lambda) \beta - \Lambda \beta) \\ &= H_{\Lambda, W} \mathbf{C} + X(X^T W X + \Lambda)^{-1} X^T W X \beta \\ &= H_{\Lambda, W} (\mathbf{C} + W \eta) \end{aligned}$$

Inclusion of a fixed intercept (e.g. $\eta_0 = \text{logit}(\bar{Y})$) has no impact on the above, as it would not be part of \mathbf{H} and \mathbf{g} .

13 Appendix: Prior sample weights

Suppose we wish to include prior sample weights in the penalized likelihood. So the optimization criterion becomes:

$$\operatorname{argmax}_{\boldsymbol{\beta}} \sum_{i=1}^n v_i \ell(\boldsymbol{\beta}; X_i, Y_i) - \boldsymbol{\beta}^T \Lambda \boldsymbol{\beta}.$$

Denote $V = \operatorname{diag}((v_i)_{i=1}^n)$. Then, from (20) we trivially have:

$$\begin{aligned} \mathbf{H} &= -X^T V W X - \Lambda = -\tilde{X}^T \tilde{W} \tilde{X} - \Lambda, \\ \mathbf{g} &= X^T V \mathbf{C} - \Lambda \boldsymbol{\beta} = \tilde{X}^T \mathbf{C} - \Lambda, \end{aligned} \tag{21}$$

with $\tilde{X} = V^T X = VX$, $\tilde{W} = WV^{-1}$. Since the Hessian and gradient are of the exact same form as in (20), Algorithm 1, and all the presented computational shortcuts also apply in this case.

14 Appendix: Proof for unpenalized covariates

Write (7) as $H_{W,\Lambda} = X(X^T W X + \Lambda')^{-1} X^T = W^{-1/2} X_W (X_W^T X_W + \Lambda')^{-1} X_W^T W^{-1/2}$. We now derive Proposition 1: an alternative, computationally efficient, expression for $H_{W,\Lambda}$. For notational convenience we first drop the W index for matrices. Define:

$$X \in \mathbb{R}^{n \times p}, X_1 \in \mathbb{R}^{n \times p_1}, X_2 \in \mathbb{R}^{n \times p_2}, \text{ s.t. } X = [X_1 | X_2],$$

and such that X_1 contains the covariates left unpenalized and X_2 the covariates to be penalized. Therefore, we write the penalty matrix Λ' , which is rank deficient, as the two-by-two block matrix containing blocks of all zeros and a $p_2 \times p_2$ penalty matrix of full rank:

$$\Lambda' = \begin{bmatrix} \Lambda_{11} & \Lambda_{12} \\ \Lambda_{21} & \Lambda_{22} \end{bmatrix} = \begin{bmatrix} \mathbf{0}_{p_1 \times p_1} & \mathbf{0}_{p_1 \times p_2} \\ \mathbf{0}_{p_2 \times p_1} & \Lambda. \end{bmatrix} \tag{22}$$

Furthermore, assume that X_1 has linearly independent columns, i.e. $\operatorname{rank}(X_1) = p_1 \leq n$ (which is reasonable as one would not include two predictors that are perfectly collinear as unpenalized covariates).

14.1 Goal

We are interested to represent the following matrix, $L \in \mathbb{R}^{p \times n}$ consisting of the matrices $L_1 \in \mathbb{R}^{p_1 \times n}$ and $L_2 \in \mathbb{R}^{p_2 \times n}$, in low-dimensional space n :

$$L := \begin{bmatrix} L_1 \\ L_2 \end{bmatrix} := (X^T X + \Lambda')^{-1} X^T = \begin{bmatrix} X_1^T X_1 & X_1^T X_2 \\ X_2^T X_1 & X_2^T X_2 + \Lambda \end{bmatrix}^{-1} \begin{bmatrix} X_1^T \\ X_2^T \end{bmatrix} \tag{23}$$

14.2 Result

Define:

$$P_1 = I_{n \times n} - X_1 (X_1^T X_1)^{-1} X_1^T,$$

which is the orthogonal projector onto the kernel (or null space) of X_1^T , or equivalently on the orthogonal complement of the column space of X_1 . Then, L_1, L_2 are given by:

$$L_1 = (X_1^T X_1)^{-1} X_1^T (I_{n \times n} - X_2 L_2) \quad (24)$$

$$L_2 = (\Lambda^{-1} - \Lambda^{-1} X_2^T (I_{n \times n} + P_1 X_2 \Lambda^{-1} X_2^T)^{-1} P_1 X_2 \Lambda^{-1}) X_2^T P_1. \quad (25)$$

14.3 Derivation

In deriving the expressions, we use two lemmas given below; the two by two block matrix inversion lemma and Woodbury's inversion lemma.

Lemma 14.1 (*two by two block matrix inversion*)

$$\begin{bmatrix} A & B \\ C & D \end{bmatrix}^{-1} = \begin{bmatrix} A^{-1} + A^{-1} B (D - C A^{-1} B)^{-1} C A^{-1} & -A^{-1} B (D - C A^{-1} B)^{-1} \\ -(D - C A^{-1} B)^{-1} C A^{-1} & (D - C A^{-1} B)^{-1} \end{bmatrix}$$

Lemma 14.2 (*Woodbury's matrix inversion, for singular C*)

$$(A + B C D)^{-1} = A^{-1} - A^{-1} B (I + C D A^{-1} B)^{-1} C D A^{-1}$$

Use the two by two block matrix inversion lemma with

$$A := X_1^T X_1, \quad B := X_1^T X_2, \quad C := B^T, \quad D := X_2^T X_2 + \Lambda$$

Define P_1 as above; $P_1 = I_{n \times n} - X_1 (X_1^T X_1)^{-1} X_1^T$. Then we find:

$$\begin{aligned} L_1 &= (A^{-1} + A^{-1} B (D - C A^{-1} B)^{-1} C A^{-1}) X_1^T + (-A^{-1} B (D - C A^{-1} B)^{-1}) X_2^T \\ &= \left[A^{-1} + A^{-1} X_1^T X_2 (X_2^T X_2 + \Lambda - X_2^T X_1 A^{-1} X_1^T X_2)^{-1} X_2^T X_1 A^{-1} \right] X_1^T \\ &\quad - \left[A^{-1} X_1^T X_2 (X_2^T X_2 + \Lambda - X_2^T X_1 A^{-1} X_1^T X_2)^{-1} \right] X_2^T \\ &= A^{-1} X_1^T + A^{-1} X_1^T X_2 (X_2^T X_2 + \Lambda - X_2^T X_1 A^{-1} X_1^T X_2)^{-1} X_2^T \\ &\quad \cdot (X_1 A^{-1} X_1^T - I_{n \times n}) \\ &= A^{-1} X_1^T \left[I_{n \times n} + X_2 (\Lambda + X_2^T (I_{n \times n} - X_1 A^{-1} X_1^T) X_2)^{-1} X_2^T \right. \\ &\quad \left. \cdot (X_1 A^{-1} X_1^T - I_{n \times n}) \right] \\ &= A^{-1} X_1^T (I_{n \times n} - X_2 (\Lambda + X_2^T P_1 X_2)^{-1} X_2^T P_1) \\ &= (X_1^T X_1)^{-1} X_1^T (I_{n \times n} - X_2 L_2) \\ L_2 &= -(D - C A^{-1} B)^{-1} C A^{-1} X_1^T + (D - C A^{-1} B)^{-1} X_2^T \\ &= -(D - C A^{-1} B)^{-1} X_2^T X_1 (X_1^T X_1)^{-1} X_1^T + (D - C A^{-1} B)^{-1} X_2^T \\ &= (D - C A^{-1} B)^{-1} X_2^T (I_{n \times n} - X_1 (X_1^T X_1)^{-1} X_1^T) \\ &= (X_2^T X_2 + \Lambda - X_2^T X_1 (X_1^T X_1)^{-1} X_1^T X_2)^{-1} X_2^T (I_{n \times n} - X_1 (X_1^T X_1)^{-1} X_1^T) \\ &= (X_2^T (I_{n \times n} - X_1 (X_1^T X_1)^{-1} X_1^T) X_2 + \Lambda)^{-1} X_2^T (I_{n \times n} - X_1 (X_1^T X_1)^{-1} X_1^T) \\ &= (X_2^T P_1 X_2 + \Lambda)^{-1} X_2^T P_1 \\ &= (\Lambda^{-1} - \Lambda^{-1} X_2^T (I_{n \times n} + P_1 X_2 \Lambda^{-1} X_2^T)^{-1} P_1 X_2 \Lambda^{-1}) X_2^T P_1, \end{aligned}$$

where the last equality follows from Woodbury's matrix inversion lemma.

Now, we apply the results for $L1, L2$ to matrices $X_{1,W} = W^{1/2}X_1$ and $X_{2,W} = W^{1/2}X_2$, and denote results for these matrices by subscript W . First, let

$$\Gamma_{W,\Lambda} = X_{2,W}\Lambda^{-1}X_{2,W}^T = W^{1/2}X_2\Lambda^{-1}X_2^TW^{1/2} = W^{1/2}\left(\sum_{b=1}^B\lambda_b^{-1}\Sigma_{2,b}\right)W^{1/2}, \quad (26)$$

with $\Sigma_{2,b} = X_{2,b}^TX_{2,b}$.

Then,

$$\begin{aligned} H_{W,\Lambda} &= W^{-1/2}X_W(X_W^TX_W + \Lambda')^{-1}X_W^TW^{-1/2} \\ &= H_{1,W,\Lambda} + H_{2,W,\Lambda} \\ &= W^{-1/2}X_{1,W}L_{1,W,\Lambda}W^{-1/2} + W^{-1/2}X_{2,W}L_{2,W,\Lambda}W^{-1/2} \\ &= W^{-1/2}X_{1,W}(X_{1,W}^TX_{1,W})^{-1}X_{1,W}^T(I_{n \times n} - X_{2,W}L_{2,W,\Lambda})W^{-1/2} \\ &\quad + W^{-1/2}X_{2,W}L_{2,W,\Lambda}W^{-1/2} \\ &= W^{-1/2}X_{1,W}(X_{1,W}^TX_{1,W})^{-1}X_{1,W}^T(I_{n \times n} - W^{1/2}H_{2,W,\Lambda}W^{1/2})W^{-1/2} \\ &\quad + H_{2,W,\Lambda}, \end{aligned} \quad (27)$$

with:

$$\begin{aligned} H_{2,W,\Lambda} &= W^{-1/2}X_{2,W}L_{2,W,\Lambda}W^{-1/2} \\ &= W^{-1/2}X_{2,W}\left(\Lambda^{-1} - \Lambda^{-1}X_{2,W}^T(I_{n \times n} + P_{1,W}X_{2,W}\Lambda^{-1}X_{2,W}^T)^{-1}P_{1,W}X_{2,W}\Lambda^{-1}\right) \\ &\quad \cdot X_{W,2}^TP_{1,W}W^{-1/2} \\ &= W^{-1/2}\Gamma_{W,\Lambda}P_{1,W}W^{-1/2} - W^{-1/2}\Gamma_{W,\Lambda}(I_{n \times n} + P_{1,W}\Gamma_{W,\Lambda})^{-1}P_{1,W}\Gamma_{W,\Lambda}P_{1,W}W^{-1/2} \\ &= W^{-1/2}\Gamma_{W,\Lambda}\left(I_{n \times n} - (I_{n \times n} + P_{1,W}\Gamma_{W,\Lambda})^{-1}P_{1,W}\Gamma_{W,\Lambda}\right)P_{1,W}W^{-1/2}, \end{aligned}$$

which completes the proof.

15 Appendix: Prediction and estimation of coefficients

In line with the expression for $H_{W,\Lambda}$ (27) a prediction hat matrix $H_{W,\Lambda}^{\text{new}} = X^{\text{new}}(X^TWX + \Lambda')^{-1}X^T$ is easily computed:

$$H_{W,\Lambda}^{\text{new}} = X_1^{\text{new}}K_{W,\Lambda} + \Gamma_{\Lambda}^{\text{new}}M_{W,\Lambda}, \quad (28)$$

where

$$\Gamma_{\Lambda}^{\text{new}} = \sum_{b=1}^B\lambda_b^{-1}\Sigma_{2,b}^{\text{new}}, \quad \Sigma_{2,b}^{\text{new}} = X_{2,b}^{\text{new}}(X_{2,b})^T,$$

$$K_{W,\Lambda} = (X_{1,W}^TX_{1,W})^{-1}X_{1,W}^T\left(I_{n \times n} - W^{1/2}H_{2,W,\Lambda}W^{1/2}\right)W^{-1/2}$$

and

$$M_{W,\Lambda} = W^{1/2}\left(I_{n \times n} - (I_{n \times n} + P_{1,W}\Gamma_{W,\Lambda})^{-1}P_{1,W}\Gamma_{W,\Lambda}\right)P_{1,W}W^{-1/2}.$$

Here, $K_{W,\Lambda}$ and $M_{W,\Lambda}$ are $p_1 \times n$ and $n \times n$ matrices (with $p_1 < n$) available from the fitting, as part of $H_{W,\Lambda}$, which are easily stored. In addition, the n vector containing the final linearized response $\mathbf{L} = \mathbf{C} + W\boldsymbol{\eta}$ (8) of the IWLS algorithm needs to be stored to compute linear predictors for the new samples: $\boldsymbol{\eta}_{W,\Lambda}^{\text{new}} = H_{W,\Lambda}^{\text{new}}\mathbf{L}$.

For estimation of $\boldsymbol{\beta}$, we use that $X\boldsymbol{\beta}_\Lambda = H_{W,\Lambda}\mathbf{L}$, and analogous to (28) we have

$$H_{W,\Lambda} = X_1 K_{W,\Lambda} + X_2 \Lambda^{-1} X_2^T M_{W,\Lambda} = X \begin{bmatrix} K_{W,\Lambda} \\ \Lambda^{-1} X_2^T M_{W,\Lambda} \end{bmatrix}.$$

Therefore,

$$\hat{\boldsymbol{\beta}}_\Lambda = \begin{bmatrix} K_{W,\Lambda} \\ \Lambda^{-1} X_2^T M_{W,\Lambda} \end{bmatrix} \mathbf{L}.$$

16 Appendix: Cox ridge

In Cox survival regression, the outcome $Y_i = (t_i, d_i)$, $i = 1, \dots, n$ denotes at which time t_i an event occurred, $d_i = 1$, or was censored, $d_i = 0$. Details for fitting Cox ridge regression by Newton updating (and hence IWLS) are given in (Van Houwelingen et al., 2006). For the use of the IWLS algorithm, it suffices to replace the CVL (3) by the cross-validated Cox likelihood (Van Houwelingen et al., 2006) and update W and C ; all other formulas remain unchanged. Note that, as outlined by Meijer and Goeman (2013), it is convenient to use the *full* log-likelihood, and not the partial one, because the latter renders a non-diagonal weight matrix. The penalized full log-likelihood is:

$$\ell(\boldsymbol{\beta}; \mathbf{Y}, X, \Lambda) = \sum_{i=1}^n (d_i(\log(h_0(t_i)) + \boldsymbol{\eta}_i) - H_0(t_i) \exp(\boldsymbol{\eta}_i)) - \frac{1}{2} \sum_{b=1}^B \lambda_b \|\boldsymbol{\beta}_b\|_2^2, \quad (29)$$

with linear predictor $\boldsymbol{\eta}_i = X_i \boldsymbol{\beta}$. As for the GLM case, $\ell(\cdot)$ is maximized by use of the IWLS algorithm, analogous to (4) to (8). In this case, updating of the baseline hazard is also required. First, denote the hazard function for individual i by $h_i(t)$, which by assumption is proportional to a baseline hazard $h_0(t)$ with cumulative hazard $H_0(t)$:

$$h_i(t) = h_0(t) \exp(\boldsymbol{\eta}_i), \quad H_0(t) = \int_{s=0}^t h_0(s) ds. \quad (30)$$

The IWLS algorithm for maximizing (29) then becomes:

$$\hat{H}_0(t) = \sum_{i: t_i \leq t} \hat{h}_0(t_i), \quad \hat{h}_0(t_i) = d_i \left(\sum_{j: t_j \geq t_i} \exp(\boldsymbol{\eta}_j) \right)^{-1} \quad (\text{Breslow estimator}) \quad (31)$$

$$W = \text{diag}((w_i)_{i=1}^n), \quad w_i = H_0(t_i) \exp(\boldsymbol{\eta}_i) \quad (\text{sample weights}) \quad (32)$$

$$\mathbf{C} = (c_i)_{i=1}^n, \quad c_i = d_i - w_i, \quad (\text{centered response vector}) \quad (33)$$

$$H_{\Lambda,W} = X(\Lambda + X^T W X)^{-1} X^T \quad (\text{hat matrix}) \quad (34)$$

$$\boldsymbol{\eta}^{\text{update}} = \boldsymbol{\eta}_{\Lambda,W}^{\text{update}} = H_{\Lambda,W}(\mathbf{C} + W\boldsymbol{\eta}) \quad (\text{linear predictor update}). \quad (35)$$

As before, this depends only on the linear predictor $\boldsymbol{\eta}$, not on $\boldsymbol{\beta}$.

17 Appendix: Functionality of the `multiridge` package

The `multiridge` package has the following functionalities:

- Fit of multi-lambda ridge by IWLS algorithm for linear, logistic and Cox ridge regression
- Inclusion of non-penalized covariates
- Fast SVD-based CV per data type to initialize multi-lambda optimization
- Optimization of Λ using any of the following criteria, all cross-validated: log-likelihood (all), AUC (binary), mean-squared error (linear, binary), c-index (survival)
- Prediction on new samples, and computation of final coefficients $\hat{\beta}_{\Lambda}$ for converged Λ
- Two-stage preferential ridge
- Paired ridge, which can be combined with multi-lambda ridge such that two data types are paired
- Repeated cross-validation for penalty parameter tuning
- Double (repeated) cross-validation for performance evaluation

Dependencies are:

- `penalized`: performing single-lambda CV after SVD (for initialization)
- `pROC` and `risksetROC`: computing performance metrics AUC and c-index for binary and survival response, respectively.
- `snowfall`: parallel computing

18 Appendix: Details about the data

Below we give further details on the data used in this paper and in the `multiridge` package.

18.1 TCGA data

Overall survival, miRNA, mRNA and CNV data was retrieved from The Cancer Genome Atlas (<https://tcga-data.nci.nih.gov/tcga/>) using `TCGAbiolinks` (Colaprico et al., 2015). We considered all complete samples from the following tumor types:

- Mesothelioma (MESO; Cancer Genome Atlas Research Network et al., 2018b), $n = 84$
- Kidney renal clear cell carcinoma (KIRC; Cancer Genome Atlas Research Network et al., 2013), $n = 506$
- Sarcoma (SARC; Cancer Genome Atlas Research Network et al., 2017), $n = 253$
- Thymoma (THYM; Cancer Genome Atlas Research Network et al., 2018a), $n = 118$

Data was preprocessed as described previously in Rauschenberger et al. (2019).

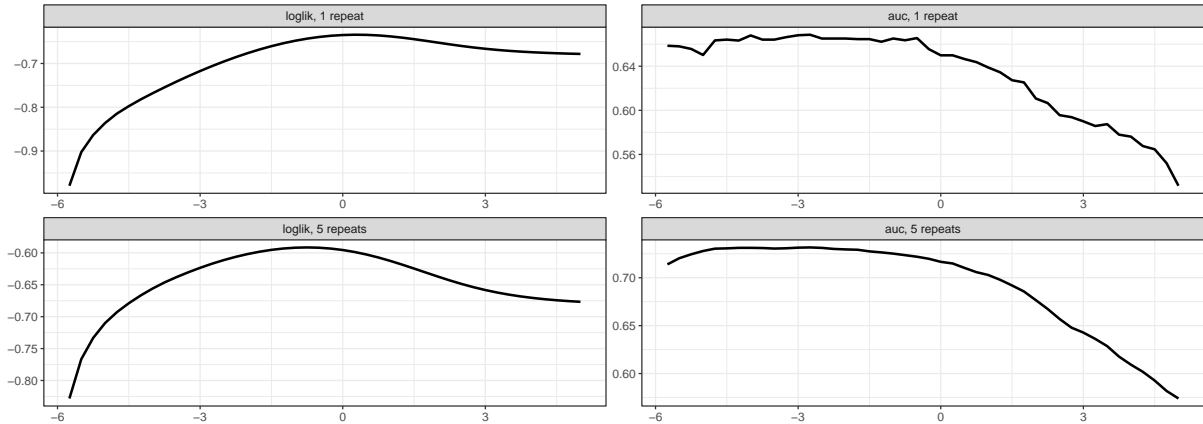


Figure 5: Profile plots showing relative penalty parameter (log-scale; x-axis) versus cross-validated performance (log-likelihood, AUC; y-axis), using either one or five repeats of 5-fold CV. Penalty parameter relative to the one optimized for log-likelihood using 1 repeat.

18.2 Cervical cancer data

For the cervical cancer data, we retrieved molecular data corresponding to two class labels: controls and cases. Here, the cases are women with a last-stage precursor lesion for cervical cancer, a so-called cervical intraepithelial neoplasia, stage 3 (CIN3). Whereas lower-grade precursor lesions are known to regress back to normal, this higher grade has a relatively high risk to progress to cancer, and is therefore usually surgically removed. Hence, control versus CIN3 is the relevant classification problem. The molecular data were obtained from self-samples, as described in Verlaat et al. (2018) for methylation and in Snoek et al. (2019) for miRNA, which both include details on the data preprocessing. We matched the molecular samples from the same individuals, rendering $n = 43$ samples (25 controls and 18 cases) for which both molecular data types were available.

19 Appendix: Profile plot for CVL and AUC

We used logistic ridge for methylation data presented in Verlaat et al. (2018) ($n = 43$, $p = 365, 620$) to illustrate profile plots of cross-validated log-likelihood and AUC as a function of λ . Figure 5 shows that the latter is not smooth when only one repeat of CV is used, but this can be countered by increasing the number of CV repeats.

20 Multi-penalty Bayesian probit regression

21 Expression for the elbo

The evidence lower bound, denoted by $\underline{p}(\mathbf{Y}; q)$, is given in Ormerod and Wand (2010), and can be rewritten in low-dimensional computations as well, using that $\boldsymbol{\mu}_{q(\beta)} = (X^T X +$

$\Lambda)^{-1}X^T\boldsymbol{\mu}_{q(a)}$ after convergence of the algorithm:

$$\begin{aligned}
\underline{p}(\mathbf{Y}; q) &= \mathbf{Y}^T \log(\Phi(\boldsymbol{\mu}_{q(\eta)})) + (\mathbf{1}_n - \mathbf{Y})^T \log(\mathbf{1}_n - \Phi(\boldsymbol{\mu}_{q(\eta)})) \\
&\quad - \frac{1}{2} \boldsymbol{\mu}_{q(a)}^T X (X^T X + \Lambda)^{-1} \Lambda (X^T X + \Lambda)^{-1} X^T \boldsymbol{\mu}_{q(a)} \\
&\quad - \frac{1}{2} \log |\Lambda^{-1} X^T X + I_{p \times p}| \\
&= \mathbf{Y}^T \log(\Phi(\boldsymbol{\mu}_{q(\eta)})) + (\mathbf{1}_n - \mathbf{Y})^T \log(\mathbf{1}_n - \Phi(\boldsymbol{\mu}_{q(\eta)})) \\
&\quad - \frac{1}{2} \boldsymbol{\mu}_{q(a)}^T H_\Lambda (I_{n \times n} - H_\Lambda) \boldsymbol{\mu}_{q(a)} - \frac{1}{2} \log |X \Lambda^{-1} X^T + I_{n \times n}| \\
&= \mathbf{Y}^T \log(\Phi(\boldsymbol{\mu}_{q(\eta)})) + (\mathbf{1}_n - \mathbf{Y})^T \log(\mathbf{1}_n - \Phi(\boldsymbol{\mu}_{q(\eta)})) \\
&\quad - \frac{1}{2} \boldsymbol{\mu}_{q(a)}^T H_\Lambda (I_{n \times n} - H_\Lambda) \boldsymbol{\mu}_{q(a)} - \frac{1}{2} \log |\Gamma_\Lambda + I_{n \times n}|,
\end{aligned} \tag{36}$$

with Γ_Λ as in Equation (10). Here we used Sylvester's determinant identity Press (2005) and:

$$\begin{aligned}
&X(X^T X + \Lambda)^{-1} \Lambda (X^T X + \Lambda)^{-1} X^T \\
&= X(X^T X + \Lambda)^{-1} (X^T X + \Lambda - X^T X) (X^T X + \Lambda)^{-1} X^T \\
&= X(I - (X^T X + \Lambda)^{-1} X^T X) (X^T X + \Lambda)^{-1} X^T \\
&= H_\Lambda - H_\Lambda H_\Lambda = H_\Lambda (I_{n \times n} - H_\Lambda).
\end{aligned}$$

21.1 Expression for CPO

The conditional predictive ordinate on log-level equals

$$\begin{aligned}
\text{CPO}_{\log} &= \frac{1}{n} \sum_{i=1}^n \log(\text{CPO}_i), \text{ with:} \\
\text{CPO}_i^{-1} &= \frac{1}{\pi(Y_i | \mathbf{Y}_{-i})} = \frac{\pi(\mathbf{Y}_{-i})}{\pi(\mathbf{Y})} = \int_{\eta_i} \frac{\pi(\mathbf{Y}_{-i} | \eta_i) \pi(\eta_i)}{\pi(\mathbf{Y})} d\eta_i \\
&= \int_{\eta_i} \frac{\pi(\mathbf{Y} | \eta_i) / \pi(Y_i | \eta_i) \pi(\eta_i)}{\pi(\mathbf{Y})} d\eta_i = \int_{\eta_i} \frac{\pi(\eta_i | \mathbf{Y})}{\pi(Y_i | \eta_i)} d\eta_i.
\end{aligned} \tag{37}$$

Here, the posterior $\pi(\eta_i | \mathbf{Y})$, with $\eta_i = \mathbf{X}_i \hat{\boldsymbol{\beta}}_{-i}^{\hat{\Lambda}(-i)}$, follows directly from the Gaussian posterior of $\hat{\boldsymbol{\beta}}_{-i}^{\hat{\Lambda}(-i)}$ (Ormerod and Wand, 2010), where the empirical Bayes estimate of Λ , obtained by maximizing the elbo $\underline{p}(\mathbf{Y}; q)$ (36), and the posterior estimate of $\boldsymbol{\beta}$ are obtained without use of sample i . So, computation of CPO only requires one-dimensional numerical integration on top of the fast VB-EB method which combines fast approximation of $\pi(\eta_i | \mathbf{Y})$ by Algorithm 2 with efficient computation (and maximization) of the elbo using (36). As defined in (37) CPO_{\log} mimics leave-one-out-cross-validation, but this may straightforwardly be extended to k -fold CV, which will imply an additional speed-up of the algorithm, as fewer fits are required. Finally, posterior $\pi(\eta_i | \mathbf{Y})$ depends on the cross-validated versions of H_Λ and Γ_Λ , which are efficiently computed from (16) and (17).

References

Aben, N. et al. (2016). TANDEM: a two-stage approach to maximize interpretability of drug response models based on multiple molecular data types. *Bioinformatics*, **32**, i413–i420.

- Bernau, C. et al. (2014). Cross-study validation for the assessment of prediction algorithms. *Bioinformatics*, **30**, i105–i112.
- Bondell, H. and Reich, B. (2012). Consistent high-dimensional bayesian variable selection via penalized credible regions. *J. Amer. Statist. Assoc.*, **107**, 1610–1624.
- Boulesteix, A.L. et al. (2017). IPF-LASSO: Integrative-penalized regression with penalty factors for prediction based on multi-omics data. *Comp. Math. Meth. Med.*, **2017**.
- Boyle, E.A. et al. (2017). An expanded view of complex traits: From polygenic to omnigenic. *Cell*, **169**, 1177–1186.
- Broët, P. et al. (2009). Prediction of clinical outcome in multiple lung cancer cohorts by integrative genomics: implications for chemotherapy selection. *Cancer research*, **69**, 1055–1062.
- Cancer Genome Atlas Research Network et al. (2013). Comprehensive molecular characterization of clear cell renal cell carcinoma. *Nature*, **499**, 43.
- Cancer Genome Atlas Research Network et al. (2017). Comprehensive and integrated genomic characterization of adult soft tissue sarcomas. *Cell*, **171**, 950–965.
- Cancer Genome Atlas Research Network et al. (2018a). The integrated genomic landscape of thymic epithelial tumors. *Cancer Cell*, **33**, 244–258.
- Cancer Genome Atlas Research Network et al. (2018b). Integrative molecular characterization of malignant pleural mesothelioma. *Cancer Discovery*, **8**, 1548–1565.
- Chaturvedi, N. et al. (2014). Fused lasso algorithm for Cox proportional hazards and binomial logit models with application to copy number profiles. *Biometrical Journal*, **56**, 477–492.
- Colaprico, A. and Silva, T. et al. (2015). TCGAbiolinks: an R/Bioconductor package for integrative analysis of TCGA data. *Nucl acids res*, **44**, e71–e71.
- Dobriban, E. and Wager, S. (2018). High-dimensional asymptotics of prediction: Ridge regression and classification. *The Annals of Statistics*, **46**, 247–279.
- Firinguetti, L. (1999). A generalized ridge regression estimator and its finite sample properties. *Communications in Statistics-Theory and Methods*, **28**, 1217–1229.
- Fong, E. and Holmes, C. (2019). On the marginal likelihood and cross-validation. *arXiv preprint arXiv:1905.08737*.
- Hastie, T. and Tibshirani, R. (2004). Efficient quadratic regularization for expression arrays. *Biostatistics*, **5**, 329–340.
- Hoerl, A.E. and Kennard, R.W. (1970). Ridge regression: Biased estimation for nonorthogonal problems. *Technometrics*, **12**, 55–67.
- Klau, S. et al. (2018). Priority-Lasso: a simple hierarchical approach to the prediction of clinical outcome using multi-omics data. *BMC bioinformatics*, **19**, 322.

- Meijer, R. and Goeman, J. (2013). Efficient approximate k-fold and leave-one-out cross-validation for ridge regression. *Biom. J.*, **55**, 141–155.
- Münch, M.M. et al. (2019). Adaptive group-regularized logistic elastic net regression. *Biostatistics*.
- Ormerod, J.T. and Wand, M.P. (2010). Explaining variational approximations. *Amer Statist*, **64**, 140–153.
- Özkale, M.R. et al. (2018). Logistic regression diagnostics in ridge regression. *Computational Statistics*, **33**, 563–593.
- Perrakis, K. et al. (2019). Scalable Bayesian regression in high dimensions with multiple data sources. *J Comput Graph Stat*, pages 1–22.
- Press, S.J. (2005). *Applied multivariate analysis: using Bayesian and frequentist methods of inference*. Courier Corporation.
- Rauschenberger, A. et al. (2019). Sparse classification with paired covariates. *Advances in Data Analysis and Classification*, pages 1–18.
- Salakhutdinov, R.R. and Hinton, G.E. (2008). Using deep belief nets to learn covariance kernels for Gaussian processes. In J.C. Platt, D. Koller, Y. Singer, and S.T. Roweis, editors, *Advances in Neural Information Processing Systems 20*, pages 1249–1256. Curran Associates, Inc.
- Snoek, B.C. et al. (2019). Genome-wide microRNA analysis of HPV-positive self-samples yields novel triage markers for early detection of cervical cancer. *International Journal of Cancer*, **144**, 372–379.
- Van de Wiel, M.A. et al. (2016). Better prediction by use of co-data: adaptive group-regularized ridge regression. *Statist. Med.*, **35**, 368–381.
- Van de Wiel, M.A. et al. (2018). Learning from a lot: Empirical Bayes in high-dimensional prediction settings. *Scand. J. Stat.*, pages 1–24.
- Van Houwelingen, H.C. et al. (2006). Cross-validated Cox regression on microarray gene expression data. *Stat. Med.*, **25**, 3201–3216.
- Veerman, J.R. et al. (2020). Estimation of variance components, heritability and the ridge penalty in high-dimensional generalized linear models. *Comm Statist Sim Comp*.
- Velten, B. and Huber, W. (2018). Adaptive penalization in high-dimensional regression and classification with external covariates using variational bayes. *arXiv preprint arXiv:1811.02962*.
- Verlaet, W. et al. (2018). Identification and validation of a 3-gene methylation classifier for hpv-based cervical screening on self-samples. *Clinical Cancer Research*, **24**, 3456–3464.
- Warnat-Herresthal, S. et al. (2020). Scalable prediction of acute myeloid leukemia using high-dimensional machine learning and blood transcriptomics. *iScience*, **23**, 100780.